índice

I. WILLIAMS (2)

A. B. HEDLEY

Dept. of Chemical Engineering and Fuel Technology
University of Sheffield — England

THE BEHAVIOUR OF DROPLETS WITHIN TURBULENT PIPE FLOW (1)

Several approaches to the calculation of the rate of deposition of particles from turbulent pipe flow onto boundary walls, are discussed. The need to consider the relationship between the eddy diffusivity of mass and momentum was indicated and quantified by experiment. The flow was assumed to be two-dimensional and was characterized by measurements of: the mean and r.m.s. fluctuating velocities respectively in the radial and axial directions as well as the fluid shear stress distribution. From the latter, the eddy diffusivity of the fluid was estimated. The measurements were made at Re No $= 1.27 \times 10^5$ and 2.64×10^4 *respectively at a pipe wall temperature of 294.0°K. Droplets of di-2-ethyl hexyl sebacate in the size range 0.54 — — 2.6 μm dia. were injected into the flow and their deposition velocities were measured, showing an increase with drop size and Re No respectively.*

The prediction of the rate of deposition of particles from a turbulent fluid on to boundary surfaces has many important applications. Examples include deposition in atomic reactors, spray dryers, particle sampling lines and in any flow system where suspended particles are transported from a generating source to the place of application.

A straight, smooth walled, cylindrical duct offers the most convenient means for studying the rate of particle deposition in turbulent flow systems. The processes by which particles deposit on a pipe wall include [1], eddy diffusion, gravity settling, thermophoresis, diffusiophoresis, electrostatic effects and inertial effects such as impaction and interception. The parameter K, which describes the deposition rate, has been defined as [2]

$$K = \frac{\text{amount of particulate deposited per cm}^2 \text{ of surface s}^{-1}}{\text{the airborne particulate concentration above the surface}}$$

The approach to the problem has usually been to evolve methods of predicting K for different systems and to correlate the predictions experimentally.

In the following investigations the following assumption was often made. The structure of the turbulent fluid in pipe flow consisted of a laminated boundary layer and a turbulent core. The boundary layer was characterized by three regions [3]:

(i) laminar sublayer, $y^+ < 5$;
(ii) buffer layer, $5 < y^+ < 30$;
(iii) main boundary layer, $y^+ > 30$,

where, y^+ is the dimensionless variable, yu_τ/ν, y is

---

(1) Presented at CHEMPOR' 75 held in Lisbon, 7-12 September 1975 at the Calouste Gulbenkian Foundation Center.

Papers presented at this International Chemical Engineering Conference can be purchased directly from Revista Portuguesa de Química (Instituto Superior Técnico, Lisboa 1, Portugal) at the following prices per volume sent by surface mail, postage included (in Portuguese Escudos):

Whole set	500
Transport processes	200
Reaction engineering	150
Environmental engineering	150
Management studies	150

This paper was presented at the Transport processes section.

(2) Present address: Shell Research Ltd., Thornton Research Centre, P. O. Box 5, Chester CH1 3SH.

the distance normal to the surface measured outwards, and u_τ is the fluid friction velocity defined as

$$u_\tau = \sqrt{(\tau_0/\rho)}. \quad (1)$$

τ_0 is the tangential shearing stress on the surface over which the fluid flows, ρ is the fluid density, and ν is the fluid kinematic viscosity.

The equation used to describe the rate R of transport of particles from the turbulent core to the wall is

$$R = (D + \varepsilon_p) dC/dy, \quad (2)$$

where D is the molecular diffusivity and ε_p is the particle eddy diffusion coefficient due to the turbulence; C is the concentration of the diffusing substance at a distance y from the surface. The particles were usually assumed to diffuse by eddy diffusion from a constant particle concentration in the turbulence core of the pipe up to, and in some theories, into, the boundary layer. In the diffusion process the eddy diffusivities of the particle and fluid were assumed equal. At the point where the eddy diffusion process was assumed to end, the particle was associated with a free flight velocity v, and a stop distance [3] ds, where $ds = v_f' \tau$ and τ is the particle relaxation time. For particles obeying Stokes law of resistance,

$$\tau = \frac{m}{6\pi r_p \eta} = \frac{2^r p^{2\rho} p}{9\eta} \quad (3)$$

where r_p is the particle radius, m the particle mass, ρ_p its density and η is the viscosity of the fluid. The value of v was usually equated to a function of the root-mean-square radial resolute of the fluid fluctuation velocity v_f'.

FRIEDLANDER and JOHNSON [4] derived deposition velocities on the basis of the above postulate. They assumed that $v = 0.9\, u_\tau$. This figure seemed unreasonably high and according to the fundamental turbulence measurements made by LAUFER [5] this velocity existed at a distance $y^+ = 80$ which was within the turbulent core and not within the boundary layer. Even using such a high initial velocity, the particle stopping distance was often less than the thickness of the laminar sublayer. This led FRIEDLANDER and JOHNSON [4] to use the hypothesis of LIN *et al.* [6] who determined the following empirical expression for ε_f, the fluid eddy diffusivity, within the laminar sublayer:

$$\varepsilon_f/\nu = (y + /14.5)^3 \quad (4)$$

According to this model, eddies from the turbulent core at a distance $y^+ = 80$, penetrated the boundary layer and retained their momentum until they were within a distance S^+, from the wall, where $S^+ = 0.9\tau^+$ and τ^+, the dimensionless particle relaxation time was equal to $\tau u^2_\tau/\nu$. A finite eddy diffusivity within the laminar layer was assumed. When S^+ was calculated using the actual values of v' at $y^+ = S^+$, transport coefficients were obtained which were four orders of magnitude lower than those found experimentally by FRIEDLANDER and JOHNSON [4].

DAVIES [7] derived a deposition scheme in which he considered both inertial deposition and deposition by Brownian diffusion. The particle radius was taken as the distance of closest approach to the deposition surface. The main difference between this theory and that mentioned previously for inertial deposition [4] was that Davies calculated his free-flight particle velocity from an analytical expression derived from the measured turbulent velocity data in fully-developed turbulent pipe flow obtained by LAUFER [5]. He determined this velocity at a distance from the wall equal to $(S^+ + a^+)$, where $a^+ = r_p \times U_\tau/\nu$, not as previously [4], in the turbulent core. LAWRENCE and HUANG [8] adapted this theory and obtained solutions valid for a cylindrical coordinate system rather than the rectangular coordinate system used by DAVIES [7]. In all the above work, re-entrainment of particles from the boundary walls was assumed to be absent. Reviews of these theories and of others [9-12] differing little from the above have been given by MONTGOMERY and CORN [13] and SEHMEL [14].

In a more recent theory, LAWRENCE and HUANG [8] considered that the size of the particles relative to the scale of the turbulence was of importance and they defined a relative entrainment factor, as

$$\alpha = ds/1, \quad (5)$$

where 1 is the fluid mixing length [15] at a point within the fluid. If this ratio was greater than

unity the concept of a particle stop distance was used; however, if the quantity, α was less than unity then the mixing length was used as a measure of the particle free flight distance. On the basis of work by TCHEN [16] and SOO and TIEN [17] the authors assumed equality of particle and fluid diffusivities but included a specification of the particle root-mean-square turbulent fluctuation velocity, $v_p'^+$, with respect to the r.m.s. fluid fluctuation velocity, $v_f'^+$, in the form of a non-linear differential equation relating the latter two quantities and the particle relaxation time in the following manner:

$$\frac{dv_p'^+}{dy^+} = \frac{1}{\tau^+}\left(1 + \frac{v_f'^+}{v_p'^+}\right). \qquad (6)$$

The authors calculated the discrete particle deposition flux for fully-developed turbulent pipe flow. The results deviated widely, as did those in all the previous work reviewed, from the small amount of experimentally obtained aerosol deposition data available from other sources.

ROUHIAINEN and STACHIEWICZ [18] used the concept of frequency response developed by HJELMFELT and MOCKROS [19] to obtain a quantitative evaluation of $\varepsilon_p/\varepsilon_F$. They showed that for 30 μm diam. particles of lycopodium spore, a fourfold increase in Reynolds number Re of the suspending fluid which caused a more than fourfold increase in ε_F, only resulted in a twofold increase in ε_p. A more important result of their work for small particles was their quantitative evaluation of the shear flow induced transverse lift force on a particle in the laminar sublayer. They considered that for a vertical flow system, if the particle radial velocity was sufficient to carry the particle to such a distance from the wall, that the particle velocity in the x coordinate direction was higher than the local stream velocity in this direction, then the lift force was directed towards the wall. For lycopodeum spheres of 2 μm diam. they calculated that for $Re > 1 \times 10^4$, the particle velocity at the edge of the sublayer such that deposition on the wall took place, was three orders of magnitude lower when considering the lift force effect than when a purely inertial mechanism was considered.

SEHMEL [1] examined the effect of removing the assumptions regarding an equality of diffusivity of the particle and fluid and an equality of particle and fluid root-mean-square turbulent fluctuation velocities. He determined what dependence these variables had upon other parameters of the problem in order that theoretical calculations agreed with the experimental data, i.e. he described the combined effect of the two parameters as an «effective eddy diffusion coefficient» and gave empirical correlations for predicting this quantity for various flow conditions. He also made deposition measurements on all surfaces of a duct and introduced a gravitational factor into the correlations.

In the last few years however, it has become possible to look at the dynamics of fluid behaviour at much smaller values of y^+ than previously and work by RUNSTADLER *et al.* [20], KIM, KLINE and REYNOLDS [21], and GRASS [22] respectively has shown a relatively unknown flow pattern near the wall in turbulent bounded flow.

Turbulence appears to be produced by a regular series of eruptions of low momentum fluid which propagate outwards through a considerable depth of boundary layer dissipating in energy as y^+ increases. A simultaneous transfer of low momentum fluid occurs towards the wall with the result that a regularly disturbed boundary layer structure is

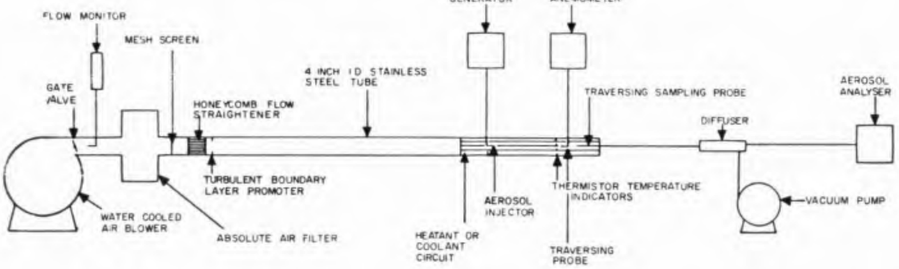

Fig. 1
A diagrammatic view of the experimental system

set up rather than the stratified laminated structure previously assumed in work on turbulent mass transfer. Measurements using hot film anemometry carried out by ECKELMAN [23] in fully developed channel flow has suggested that the fluid fluctuation velocity approaching the wall is of a similar magnitude to the friction velocity, an assumption made many years previously by FRIEDLANDER [4] though for different reasons and previously reported by REICHART [24].

Having reasonably established the transfer of momentum to a bounding wall in turbulent flow a correlation for equivalent mass transfer required that, a relationship between the ratio of the eddy diffusivity of the fluid, ε_F, to the eddy diffusivity of a particle, ε_p, and the flow properties of the fluid, was obtained.

As a first approximation it was assumed that the fluid in fully developed turbulent pipe flow fluctuated in a sinusoidal motion of frequency, f.

If it was assumed that the force, F, acting upon an entrained particle was that given by Stokes expression,

$$F = 6\pi\mu_F r_p Vr \tag{7}$$

where μ_F was the absolute viscosity of the fluid and Vr was the terminal particle velocity, then it was predicted by ROSENSCHWEIG [25] that the entrained droplet would vibrate sinusoidally with a velocity amplitude ratio of,

$$\frac{V_{particle}}{V_{fluid}} = [1 + (4\pi f r_p{}^2 \rho_p / 9\mu_F)^2]^{-\frac{1}{2}} \tag{8}$$

The above expression was solved for 1 and 5 μm diameter droplets vibrating in turbulent pipe flows of Re $= 1.27 \times 10^5$ and 2.64×10^4 respectively at the corresponding frequencies calculated for our present work, the results are given in Table 1 and show that the deviation of the relationship from unity was theoretically negligible.

It was apparent from the current state of aerosol deposition studies in turbulent flow, that certain aspects of the problem warranted further investigation; these were: (1) more experimental results of particle deposition rates from turbulent pipe flow under closely controlled conditions were needed and (2) the relationship between the particle diffusivity and the fluid diffusivity $\varepsilon_p/\varepsilon_F$ under practical conditions needed clarification.

It was decided to construct a variable flow system in which fully-developed turbulent pipe flow was achieved. An initial investigation was designed to characterize the flow in terms of the mean and fluctuating velocities U, u′, V, v′ in the axial and radial directions respectively, and to allow the determination of the shear stress, $\overline{uv}$ as a function of y and hence the eddy diffusivity of the fluid from the relationship

$$\varepsilon/\upsilon = \frac{\overline{uv}/u_\tau{}^2}{du^+/dy^+}\ , \tag{9}$$

where

$$\frac{du^+}{dy^+} = \frac{d(U/U_o)}{d(y/a)}\ \frac{U_o\upsilon}{U_\tau a U_\tau} \tag{10}$$

and a is the pipe radius, U is the mean axial velocity at a point, and U_0 is the maximum mainstream velocity at the centre line.

The measurement of the above quantities was carried out using hot-wire anemometry. Non-volatile droplets having a low surface tension of 30 MN m^{-1} were chosen as the disperse phase since in the deposition measurements mass transfer and re-entrainment from the walls respectively would be minimized. By carrying out concentration traverses of the aerosol injected into the turbulent flow, the diffusivity of the particles in the fluid was determined. The measurement of the aerosol concentration was carried out by sampling the aerosol isokinetically and using a multi-channel light-scattering counter which was developed for the purpose [26].

In this experiment the effect of charge was minimized by generating a condensation aerosol, examining it for charge using a charge analyzer and if necessary neutralizing the aerosol using a charge generator designed to produce equal numbers of $^+$ve and $^-$ve ions.

The experimental unit is shown diagrammatically in fig. 1 and consisted of three units, the flow system, the aerodynamic analysis system and the aerosol generation and analysis unit. The duct assembly consisted of a valve regulated blower

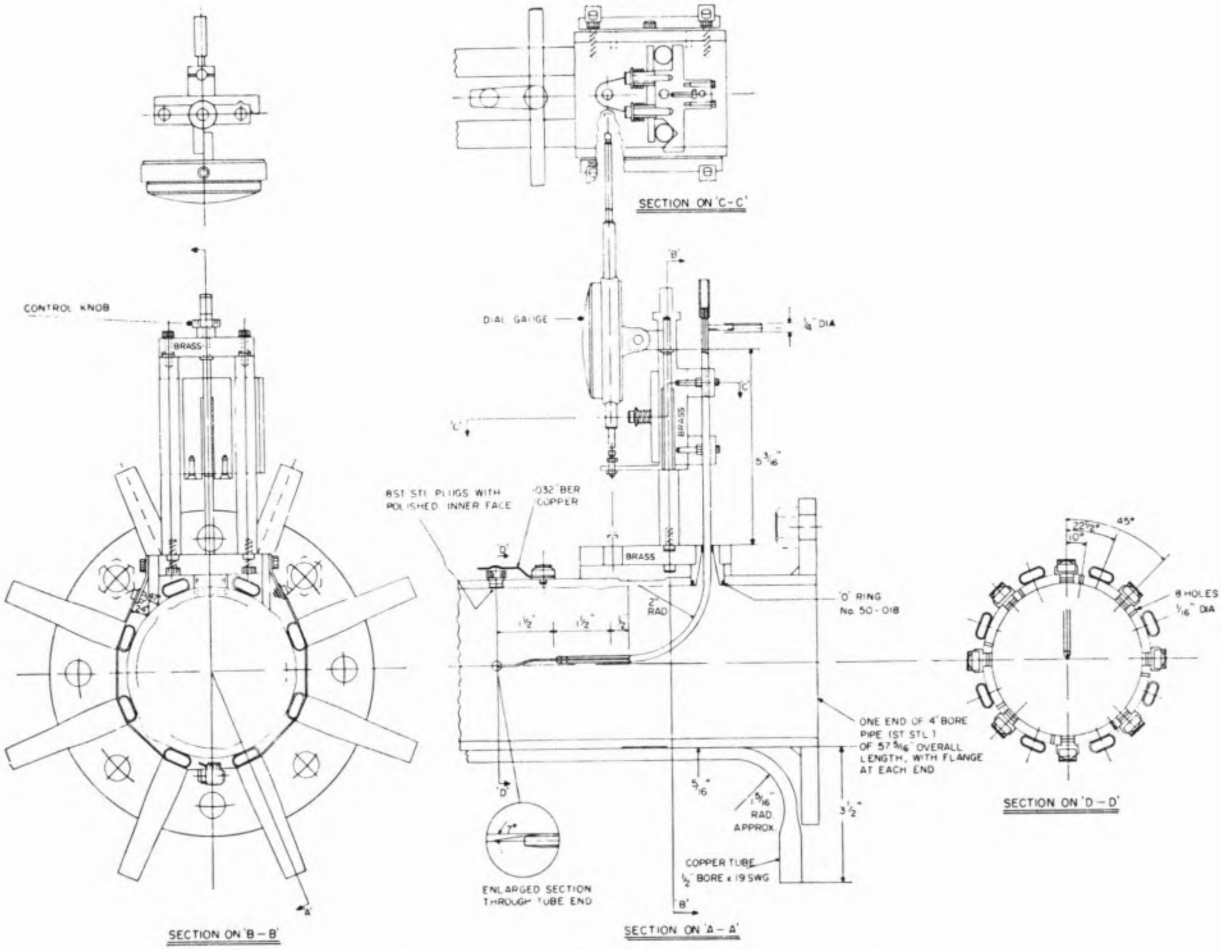

Fig. 2

Test section for turbulent pipe flow rig showing probe traversing mechanism with a pilot static tube in situ

which passed up to 0.4 $m^3\ s^{-1}$ of cooled air through an absolute filter unit, a 0.6 cm mesh screen and a 35-cm-long section of paper honeycomb into the first of six interlocking sections of 10.16 cm i.d. 154.2 cm long stainless steel tubes each of which was mirror polished internally. The turbulent boundary layer was instigated by an annular protuberance of 1.5 mm depth in the first section. Each tube was fitted with the facility to accomodate an aerosol injection point in the form of an airfoil wedge section across the duct. The last two sections of the duct acted as test sections and were fitted with 20 equispaced pressure tappings and each section had facilities for fitting a probe scanning unit shown in fig. 2. Around the periphery of the duct at the corresponding axial position to the internal probe tip, eight thermistors recorded the internal wall temperature and eight adjacent, removable plugs were fitted flush with the inside tube wall to act as droplet sample holders which were subsequently examined microscopically. The wall temperature of the last section of the duct was controlled by passing ethylene glycol through eight, 1.27 cm i.d. copper tubes fastened to the outer tube wall. The flow Reynolds number range available with the unit was between 2.64×10^4 and 1.27×10^5 with wall temperatures between 279 and 317 °K.

The second unit in the experiment a DISA hot-wire anemometer type 55D01 was used to determine the aerodynamic characteristics of the fluid flow. These quantities were the fluid shear stress $-\overline{uv}$, where u and v were the instantaneous values of velocity fluctuations in the x or y directions respectively, the mean axial velocities, U and U_0, and the root-mean-square fluctuating velocity

components in the axial and radial directions, u′ and v′. In order to determine v′, it was necessary to determine the double correlation coefficient $\overline{uv}/u'v'$. The probes used in the experiment were DISA gold-plated miniature probes, types 55F14, 55F12 and 55F11, to measure the average velocity profiles, the shear stress and the fluctuating root-mean-square velocities respectively. The correlation coefficient was measured at several points during a traverse in the test section, using a DISA cross-wire probe. In the aerodynamic measurements two dimensional duct flow was assumed.

The effect of the fluid temperature variation on the hot-wire results was taken into account by calibrating the probes at several temperatures within the range of interest. A plot of the calibration constants against the temperature was then made. For calibration purposes the DISA calibration wind tunnel was used with a modification. The air was heated or cooled by passing through an automobile radiator at the inlet to the tunnel. Ethylene glycol acted as heatant or coolant and the temperature of the air in the wind tunnel was monitored using a thermistor.

The third part of the experimental apparatus was the aerosol generation, sampling and analysis unit.

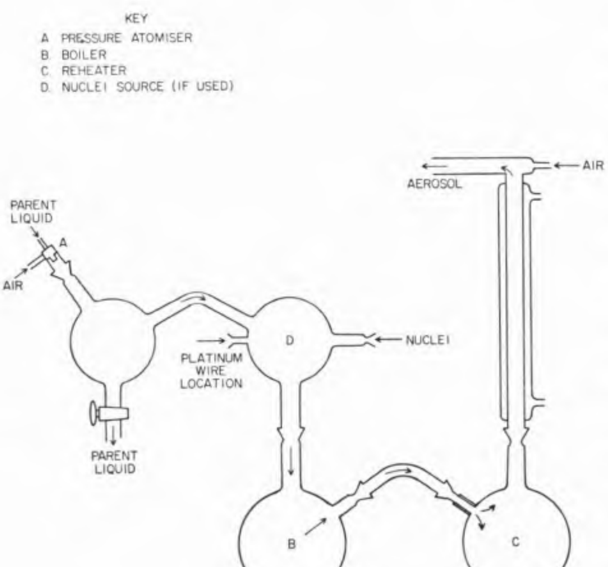

Fig. 3
The aerosol generator

The aerosol was generated from di-2-ethyl hexyl sebacate in a generator shown diagrammatically in fig. 3. This was a condensation generator, a description of which had been given previously [27]. Some modifications to the generator were made for this work. The two most important were the provision of additional flow controllers at the outlet of each gas supply and a more sophisticated temperature control system. The temperature controller incorporated an electronic proportional control circuit with a fine differential control applied. The sensor units were negative temperature coefficient thermistors which were fitted into the boiler and reheater flasks respectively. This unit enabled temperature control within ± 0.5 °C which was necessary for a reproducible aerosol. The use of a condensation generator precluded the formation of charged droplets. That this condition was satisfied was tested by passing the aerosol in a laminar air stream between two plates with a potential of 5 kV between them. The plates were examined for deposited droplets using photomicrography, and if necessary, the aerosol was neutralized by passing through a charge apparatus designed to generate equal number of $^{+}$ve and $^{-}$ve ions, both the charge analyzer and charger were designed after LANGER and RADNICK [28].

Particles were pumped through the sampling probe and then through a conical diffuser, to a sensing system where the particles were classified into ten size-ranges and total counts in each range were indicated digitally.

The anemometer hot-wire data was processed using a statistical approach to the signal analysis developed by DVORAK and SYRED [29].

This method was applied to the two-dimensional system under discussion and necessitated measurements from a straight wire probe in two 90° mutually differing positions. The equations were solved for the mean and fluctuating velocities in the axial and radial directions at a number of points on a traverse across the duct test-section.

The correlation coefficient was measured at several points across the duct using a cross-wire probe. The shear stress component was evaluated from measurements made with a 45°-slant wire probe [30] rotated through 180° by assuming that the heat transfer from the wire depended only upon the flow velocity normal to the wire.

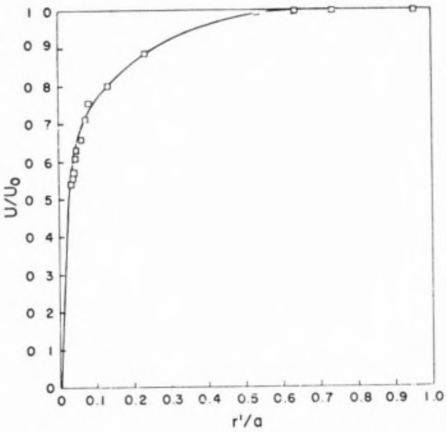

Fig. 4
The fluid velocity profile in turbulent pipe flow at $Re = 2.64 \times 10^4$

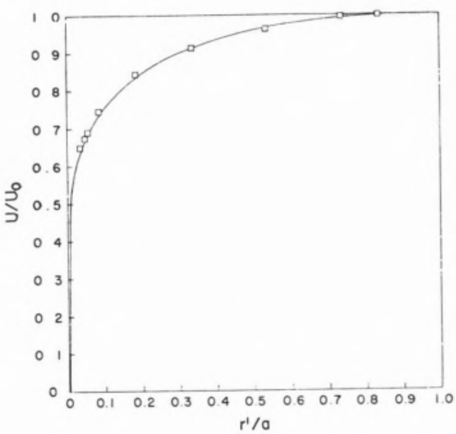

Fig. 5
The fluid velocity profile in turbulent pipe flow at $Re = 1.27 \times 10^5$

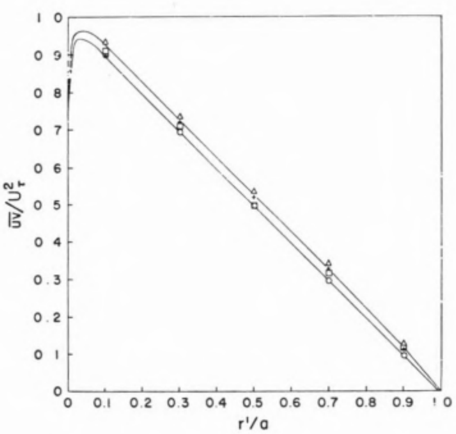

Fig. 6
The shear stress profile of turbulent pipe flow
Curve 1, $Re = 1.27 \times 10^5$; Curve 2, $Re = 2.64 \times 10^4$

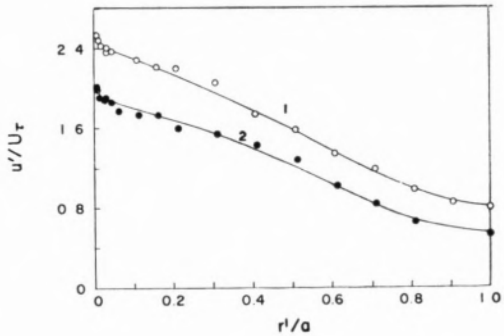

Fig. 7
The distribution of u' within turbulent pipe flow at $Re = 1.27 \times 10^5$ and 2.64×10^4 respectively
Curve 1, represents $u'/U\tau$ at $Re = 1.27 \times 10^5$
Curve 2, represents $u'/U\tau$ at $Re = 2.64 \times 10^4$

In a fully-developed pipe flow the velocity distribution across a pipe is independent of the stream wise position. Under these conditions the pressure drop along a pipe is balanced by the tangential stress, τ_0, where,

$$\tau_0 = adP/2dx \qquad (11)$$

In this experiment the static pressure tapping along the last two pipe sections enabled a measurement of dP/dx, the pressure drop, to be made and so a direct determination of the tangential wall stress was possible,

Fig. 4 shows the velocity profile across the test section, at $Re = 2.67 \times 10^4$ and fig. 5 shows similar data for $Re = 1.27 \times 10^5$.

A plot of the shear stress, non-dimensionalized with the friction velocity, as a function of r′/a is shown in fig. 6. The curves correspond to Reynolds numbers of 2.67×10^4 (upper curve) and $1.27 \times \times 10^5$ (lower curve).

The distribution of the axial root-mean-square,

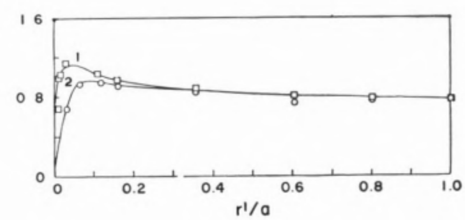

Fig. 8
The distribution of v′ within turbulent pipe flow at $R = 1.27 \times 10^5$ and 2.67×10^4 respectively
Curve 1, represents v′ at $Re = 1.27 \times 10^5$
Curve 2, represents v′ at $Re = 2.64 \times 10^4$

fluctuating, turbulent velocity component u′, non-dimensionalized with U_τ, is shown in fig. 7. The upper curve shows the distribution of a Reynolds number of 1.27×10^5 and the lower curve was determined for a Reynolds number of 2.64×10^4.

The last of the turbulent quantities, the distribution of the radial root-mean-square turbulent fluctuating velocity component, v′, is shown in fig. 8. This quantity was again non-dimensionalized with the friction velocity. The upper curve corresponds to a Reynolds number of 1.27×10^5 and the lower curve to one of 2.64×10^4.

Finally, fig. 9, shows the eddy diffusivity of the fluid in the turbulent pipe flow, non-dimensionalized

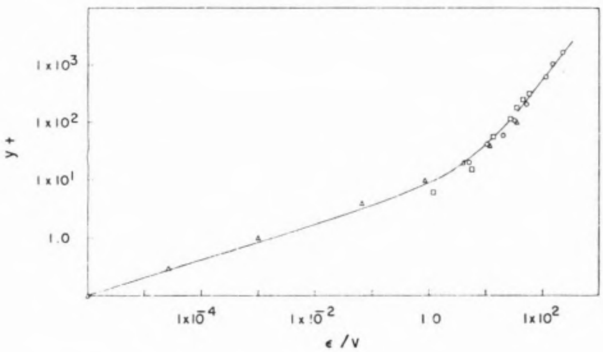

Fig. 9
The fluid eddy diffusivity distribution in turbulent pipe flow. ○, results obtained at Re = 1.27 × 10⁵; □, results obtained at Re = 2.64 × 10⁴; △, theoretically derived results from ref. (7)

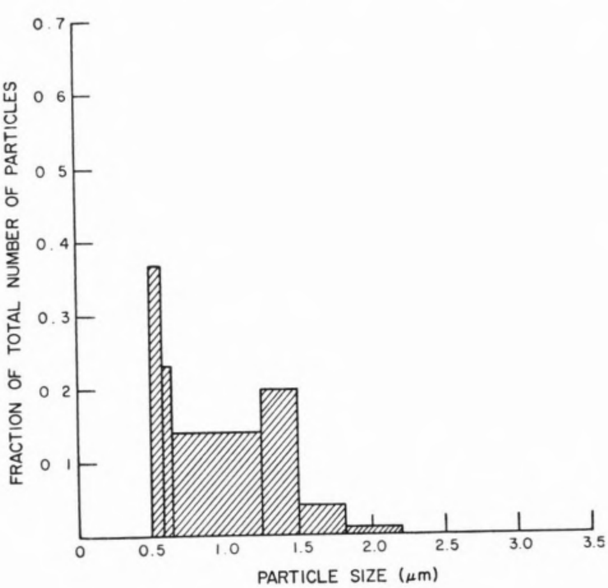

Fig. 10
Aerosol size distribution

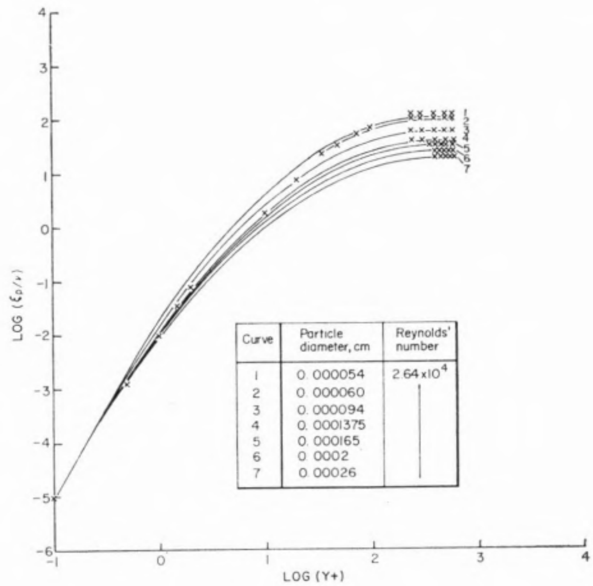

Fig. 11
Relationship between particle diffusivity and the distance from the wall of the tube

with the kinematic viscosity of air, plotted against the non-dimensional parameter y^+. The figure shows the results at Reynolds numbers of $1.27 \times$ $\times 10^5$ and 2.64×10^4 and also the theoretical points derived from Ref. 6.

With regard to the determination of the fluid dynamic characteristics of the flow in the duct,

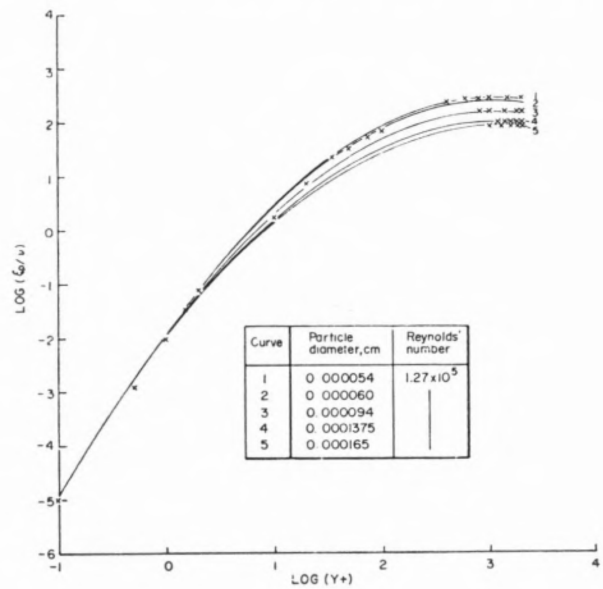

Fig. 12
Relationship between particle diffusivity and the distance from the wall of the tube

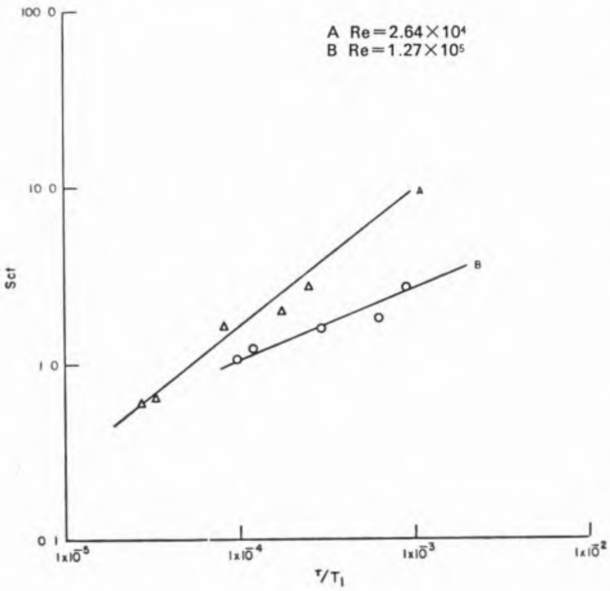

Fig. 13

The relationship between, $\tau/T_1 \dfrac{\textit{the particle relaxation time}}{\textit{fluid macro scale}}$ *and* $\xi f/\xi p$, *Sct No.*

it was necessary to determine how closely the present system approached fully-developed turbulent flow. This was indicated by several features. For both values of Reynolds number, the velocity profiles were typical, flat, turbulent profiles as opposed to the parabolic profile expected from laminar flow. The shear stress profiles shown in fig. 6 showed little dependence on Reynolds number and varied linearly across the duct cross-section.

The turbulent intensities, u'/U_0 were calculated for $r'/a = 0.1$ and 1.0 for Reynolds number of 1.27×10^5 and 2.64×10^4. The intensities were compared with those calculated by LAUFER [5] for Reynolds numbers of 5×10^5 and 5×10^4 and the comparison is shown in Table 2. The similarity of the magnitude of the turbulent intensities in the present system and those measured by LAUFER [5] at higher Reynolds numbers indicated that fully-developed turbulent flow was achieved in our system.

Having established the flow characteristics in our pipe flow system, an aerosol, consisting of droplets of di-2-ethyl hexyl sebacate suspended in air, with a constant size distribution shown in fig. 10, was introduced at the centre line of the duct through a point source injection system. The mass concentration of material leaving the injector was approximately 8×10^{-8} gm cm^{-3}.

The individual particle concentrations were determined at radially displaced locations from the tube centre line to the wall and at axial locations up to 9.0 m from the injector.

Particle eddy diffusivities were obtained from these measurements by using the relationship:

$$R_R = \frac{R_I U_o}{4\pi R_A \varepsilon_p x} \; e^{\frac{-U r_s^2}{4 \varepsilon_p x}} \qquad (12)$$

where

- R_R was the local mass ratio of droplet material to air,
- R_I was the material injection rate,
- R_A was the air mass velocity,
- x was the axial distance,

and r_s was the radial distance to the sampling position.

If the relationship r_s^2 vs R_R was plotted on semi-logarithmic coordinates then the diffusivity was obtained from the slope of the curve.

Figs. 11 and 12 show experimental measurements of, ε_p, non-dimensionalized with the fluid viscosity, ν, as a function of; the non-dimensional radial distance parameter y^+, and the particle diameter, d_p, at Re $= 2.64 \times 10^4$ and 1.27×10^5 respectively. Also shown on each figure are the theoretically predicted values of ε_p/ν, shown by solid lines, which have been derived from the following function;

$$\log \varepsilon_p/\nu = \log B_1 \mathrm{Re}^{B_2} dp^{B_3} - \\ - \log B_4 \mathrm{Re}^{B_5} dp^{B_6} (\log y^+ \mathrm{Re}^{B_7} dp^{B_8})^2 \qquad (13)$$

where $B_1 - B_8$ were constants derived from a non-linear least squares analysis of practically obtained data.

An experimentally derived relationship between the eddy diffusivities of the fluid and the particle respectively is shown in fig. 13 where the Schmidt number, Sct, $= \varepsilon_F/\varepsilon_p$, was plotted as a function of, τ/T_1, where, T_1 was the Lagrangian macroscale of the fluid turbulence which was estimated from

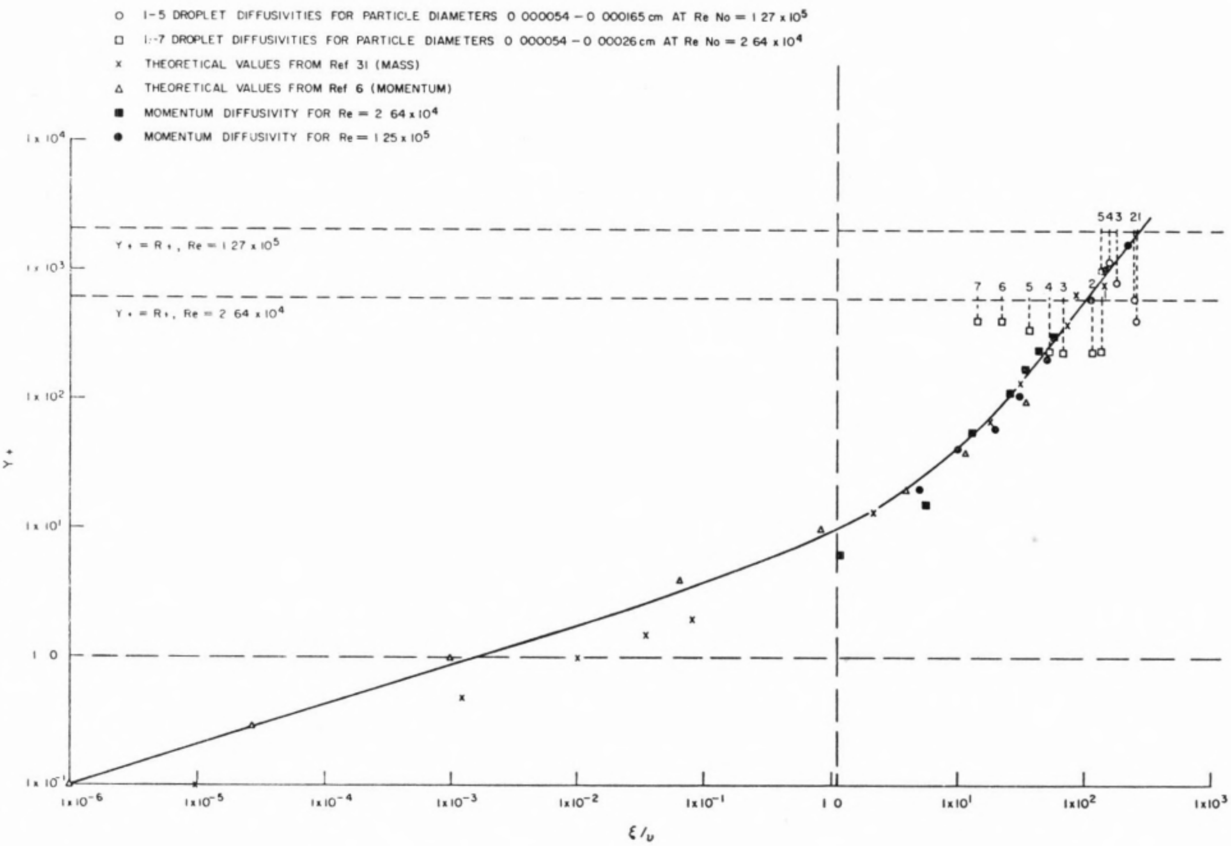

Fig. 14
The eddy diffusivities of mass and momentum

Table 1

Velocity amplitude ratio for droplets in fully developed turbulent pipe flow

Reynolds number	Particle size µm	Frequency c/s	Velocity amplification V_p/V_a
	1.0		0.9998
1.27×10^5		760.0	
	5.0		0.9174
	1.0		1.0000
2.64×10^4		188.0	
	5.0		0.9942

it's relationship to, momentum eddy diffusivity and the turbulent fluctuating velocity.

$$T_1 = \varepsilon_F/\upsilon'^2 \tag{14}$$

The particle relaxation time represented the decay with time of the velocity of a particle when it was injected into a quiescent fluid; the Lagrangian macroscale was a measure of this average time over which a fluid moved in one direction, therefore the ratio, τ/T_1, was regarded as a particle inertia parameter.

The results shown in fig. 13 indicated that as Reynolds number increased the Schmidt number decreased, which suggested that the particle diffusivity increased at a higher rate than the fluid diffusivity. The effect was reinforced by the tendency

Table 2

Comparison of relative turbulent intensities

Reynolds number	r'/a	u'/Uo	
1.27×10^5	0.1	0.079	
1.27×10^5	1.0	0.029	
2.64×10^4	0.1	0.069	
2.64×10^5	1.0	0.021	
5×10^5	0.1	0.070	(after Laufer)
5×10^5	1.0	0.027	(after Laufer)
5×10^4	0.1	0.081	(after Laufer)
5×10^4	1.0	0.027	(after Laufer)

of the macroscale to increase with an increase in Reynolds number. The results were however at variance with the simplified theoretical results shown in Table 1.

A further illustration of the deviation between the diffusivities of mass and momentum is shown in fig. 14, where experimentally obtained values of the diffusivities of a range of particle sizes from 0.000054 — 0.00026 cm at $Re = 1.27 \times 10^5$ and 2.64×10^4 respectively are shown as a function of y^+. The lower values of y^+ were obtained from a theoretical correlation suggested by HUGHMARK [31]. Also shown on the figure are our experimental diffusivities for momentum at each value of Reynolds number respectively. Extrapolation of these results to low values of y^+ was carried out using the correlation of LIN *et al.* [6]. From the work on diffusivity it was clear the eddy diffusivity in Eqn. 2 depended upon

(i) y^+
(ii) Reynolds number

and

(iii) the droplet diameter.

The deposition velocities for droplets of the following sizes:

(i) 0.000054 cm diameter
(ii) 0.000060 cm diameter
(iii) 0.000094 cm diameter
(iv) 0.0001375 cm diameter
(v) 0.000165 cm diameter
(vi) 0.0002 cm diameter

and

(vii) 0.00026 cm diameter

were determined by carrying out a mass balance along the duct at $ReNo = 1.27 \times 10^5$ and $ReNo = 2.64 \times 10^4$ respectively.

The deposition velocity, K, was calculated from the following relationship;

$$K = - [\ln (C/Co) (^{Uo}/4) (^{a}/x)] \quad (15)$$

where the droplet concentrations at the inlet and downstream positions were Co and C respectively.

Fig. 15 shows the relationship obtained between the deposition velocity and the droplet diameter at: $Re = 1.25 \times 10^5$ and 2.64×10^4 respectively with a pipe wall temperature of 294 °K.

An exponential rise in the deposition velocity with

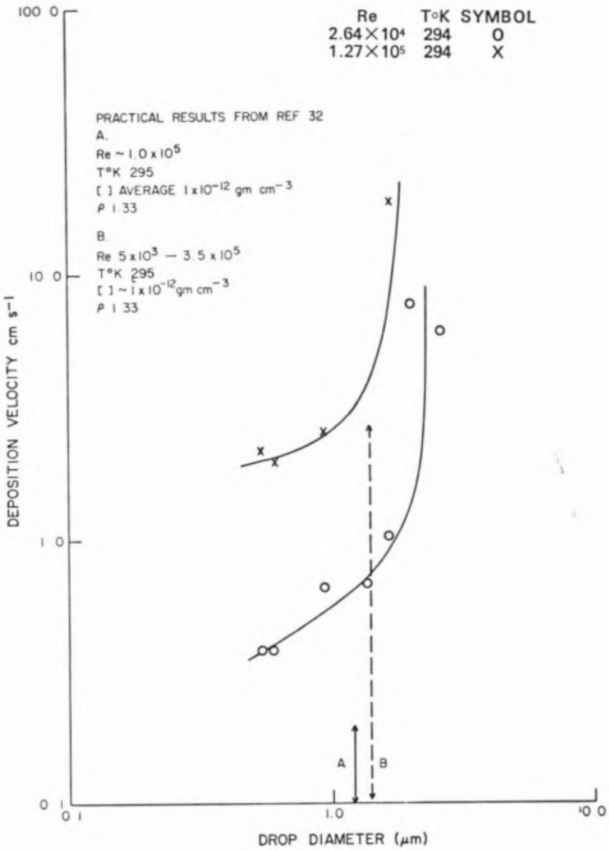

Fig. 15
Droplet deposition velocities as a function of size and concentration

an increase in this particle size was observed. For comparison, some experimentally obtained deposition velocities of $\sim 1\ \mu m$ diameter uranine particles, obtained by MONTGOMERY and CORN [32], are shown on the figure. The velocities obtained in our experiments were considerably higher, however this may have been due to the significantly higher particle mass concentrations used in our work; 8×10^{-8} gm cm^{-3} compared with 1×10^{-12} gm cm^{-8} used by MONTGOMERY and CORN [32].

Figs. 11 and 12 showed an apparent decrease in eddy diffusivity with an increase in the particle size. This may be explained as follows: if we consider the injection of a small particle at the centre line of a turbulent pipe flow system, the particle will travel towards the pipe wall.

Work by SHAW and HANRATTY [33] and POPOVICH and HUMMEL [34] respectively, has shown that low momentum fluid was continually transferred, at convective velocities approximately equal to the friction velocity, towards and away from the wall within a region:

$$0 < y^+ < 2.0$$

in turbulent boundary layer flow. It is suggested that the droplet would approach to within a distance of $\sim y^+ = 2.0$ when the eddy in which it was entrained was met by an outflow of fluid from this wall, then, at the interface of the incoming and outgoing fluids, this resultant velocity might be zero. If the particle was of the order of 0.000054 cm diameter, and the transverse fluid velocity was of the order of $0.8\ U_\tau$, then at $Re = 1.27 \times 10^5$, $ds^+ = 0.024$ so that the particle could not penetrate far into the wall region due to it's own inertia and was probably re-entrained into the core of the flow. In this way a low concentration gradient across the duct was rapidly set-up and since the effective diffusivity was an inverse function of the magnitude of this concentration gradient, a high value for ε_p resulted. If a droplet which had a diameter of 0.00026 cm had been considered, then at the interface of the fluids $ds^+ = 0.56$, so that, due to its own inertia the droplet travelled well into the final wall region where, statistically, the probability of it reaching the wall due to entrainment by fluid returning to the wall in this highly perturbed region, was high.

From the foregoing it is clear that the larger particles were removed more rapidly from the turbulent core than the smaller ones, this was supported by the results shown in fig. 15, the effect was manifested in a high radial concentration gradient with a consequent low eddy diffusivity value. In conclusion, measurements of the eddy diffusivity of mass and momentum in fully developed turbulent pipe flow have been made, and in practice the ratio, $\varepsilon_f/\varepsilon_p$ effectively increased with particle size due partly to this definition of diffusivity, but decreased with an increase in Reynolds number which indicated that the mass diffusivity increased more rapidly than momentum diffusivity under these conditions.

A theoretical relationship between the non-dimensionalized eddy diffusivity of mass, ε_p/υ, and the wall distance parameter, y^+, has been derived, as a function of:

(i) the droplet size and
(ii) Reynolds number

which appeared satisfactory within the limits,

$$1.5 < y^+ < R^+.$$

Droplet deposition velocities have been measured for a range or particle sizes and flow conditions. The deposition velocity increased with ReNo, and increased exponentially with the particle size. A tentative qualitative theory of deposition has been suggested, which was supported by the measurements that have been made.

REFERENCES

[1] SEHMEL, G. A., «Meeting Soc. Eng. Sci.», Tel Aviv, 1972.

[2] CHAMBERLAIN, A. C., *Proc. Roy. Soc. (London), Ser. A*, **290**, *236 (1966)*.

[3] DAVIES, C. N., *Aerosol Sci.*, **1**, *418 (1966)*.

[4] FRIEDLANDER, S. K. and JOHNSTONE, H. F., *Ind. Chemist*, **49**, *1151 (1957)*.

[5] LAUFER, J., «The Structure of Turbulence in Fully Developed Pipe Flow», N. A. C. A. Report, 1147, 1954.